Stochastic pitch angle diffusion due to electron-whistler wave–particle interactions

W. J. Wykes, S. C. Chapman, and G. Rowlands

Citation: Physics of Plasmas (1994-present) **8**, 2953 (2001); doi: 10.1063/1.1371953
View online: http://dx.doi.org/10.1063/1.1371953
View Table of Contents: http://scitation.aip.org/content/aip/journal/pop/8/6?ver=pdfcov
Published by the AIP Publishing

Stochastic pitch angle diffusion due to electron-whistler wave–particle interactions

W. J. Wykes,[a] S. C. Chapman,[b] and G. Rowlands
Space and Astrophysics Group, Physics Department, University of Warwick, Coventry CV4 7AL, United Kingdom

(Received 19 October 2000; accepted 23 March 2001)

In the Earth's magnetosphere, electron–whistler mode wave–particle interactions are a candidate mechanism for auroral precipitation via electron phase space diffusion. Of particular interest are stochastic interactions between relativistic electrons and (as often observed) waves of more than one wave number. It can be shown that the interaction between electrons and two oppositely directed monochromatic whistlers is stochastic. Once a threshold is exceeded, stochastic trajectories exist in addition to regular orbits (Kolmogorov–Arnold–Moser, or KAM, surfaces) near resonance, and here their corresponding pitch angle diffusion is estimated. The treatment is extended to consider broad band whistler wave packets and it is shown that the stochastic diffusion mechanism is again present for interactions with one or two wave packets. The pitch angle diffusion coefficient is estimated from the dynamics of stochastic electrons. For wave amplitudes consistent with planetary magnetospheres, such as at the Earth and Jupiter, pitch angle diffusion due to stochastic interactions occurs on fast (millisecond) time scales resulting in significant increases in the pitch angle diffusion coefficient. © *2001 American Institute of Physics.* [DOI: 10.1063/1.1371953]

I. INTRODUCTION

Electron–whistler wave–particle interactions have long been considered as a mechanism for pitch angle scattering in planetary magnetospheres. In particular gyroresonant processes with near-parallel propagating waves (e.g., Refs. 1 and 2) have been shown to produce pitch angle diffusion for electrons that are at resonance with a background of randomly phase whistler waves.[3] However, typical wave amplitudes observed in planetary magnetospheres are insufficient to result in significant phase space diffusion if only a single whistler is considered; the changes in the background field with respect to the electron mean that the resonance condition is satisfied for too short a time. Alternatively, stochasticity (in the dynamical sense), and hence stochastic diffusion, can be introduced by coupling the bounce motion of the trapped electrons with a single whistler (e.g., Ref. 4), by considering the interaction with a broad band whistler wave (e.g., Ref. 5) or by considering inhomogeneities in the medium (e.g., Ref. 6). More recently, the possibility of stochastic phase space diffusion in the presence of oppositely directed whistlers has been considered, as demonstrated numerically in Ref. 7 for a wave frequency of half the gyrofrequency and in Ref. 8 for relativistic electrons. This mechanism has been shown to exist in self-consistent simulations.[9] On closed field lines on planetary magnetospheres, oppositely directed whistlers are commonly observed as whistlers are readily reflected inside the magnetosphere.[10]

In this paper we derive the full equations of motion, for the system of two oppositely directed whistlers interacting with relativistic electrons. By initially considering monochromatic whistler waves we first show that the presence of the second wave introduces stochastic effects and then set up an analytical framework for the treatment of the more realistic case of wave packets.

We extend the treatment to consider a single wave packet, which we represent as a wave with a range of wave frequencies and wave numbers. The electron dynamics are found to be essentially the same as for a pair of monochromatic waves. It is then straightforward to consider the efficiency of the mechanism in scattering electrons for parameters consistent with a generalized planetary magnetosphere and for the interaction with two oppositely directed broad band whistler wave packets.

The degree of stochasticity in the system is quantified by estimating the Lyapunov exponents of individual trajectories. The Lyapunov exponents are shown to be positive (hence indicating stochastic trajectories) in regions of phase space where significant changes in pitch angle occur, therefore, these changes are due to stochastic effects. The Lyapunov exponents are then used to estimate the interaction time and hence the diffusion coefficient, which can be compared with the diffusion coefficient estimated using the method derived in Ref. 1 for gyroresonant processes with a single whistler.

II. MONOCHROMATIC WHISTLERS

We consider a total magnetic field, consisting of a background magnetic field, $\mathbf{B}_0 = B_0\hat{\mathbf{x}}$, and a wave field, $\mathbf{B}_\omega$. The electron population is initially in the vicinity of the magnetic equator of a magnetospheric field line, which is assumed to be uniform since, as we shall see, the electron whistler inter-

[a]Fax: +44(0)24 76692016. Electronic mail: wykes@astro.warwick.ac.uk
[b]Electronic mail: sandrac@astro.warwick.ac.uk

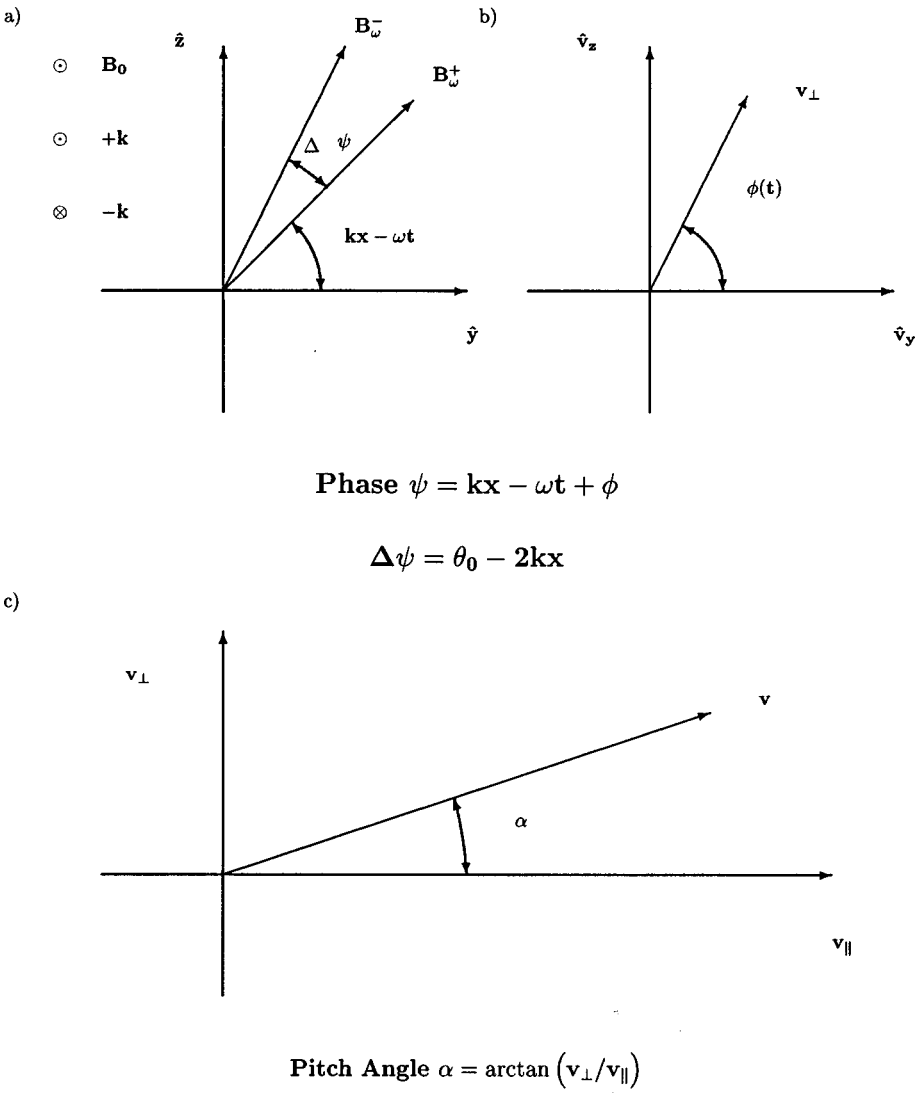

FIG. 1. Illustration of the coordinate system used in the model. In (a) the magnetic wave fields $\mathbf{B}_\omega^+$ and $\mathbf{B}_\omega^-$ lie in the $\hat{\mathbf{y}},\hat{\mathbf{z}}$ plane, perpendicular to the background field, $\mathbf{B}_0 = B_0\hat{\mathbf{x}}$. In (b) (v_y, v_z) is parameterized in terms of the perpendicular velocity, $v_\perp$, and phase, ϕ. The phase angle, $\psi = kx - \omega t + \phi$, is defined as the angle between $\mathbf{B}_\omega^+$ and the electron perpendicular velocity, $\mathbf{v}_\perp$ and the phase difference, $\Delta\psi = \theta_0 - 2kx$, is the angle between $\mathbf{B}_\omega^+$ and $\mathbf{B}_\omega^-$, where $\theta_0 = \pi$ is the initial phase difference of the waves. In (c) the electron pitch angle, α, is defined as the angle between the velocity vector $\mathbf{v}$ and the background field $\mathbf{B}_0$.

action occurs on sufficiently fast time scales such that the change in the background magnetic field experienced by the electron over the interaction time is small.

The wavefield $\mathbf{B}_\omega$ is composed of the superposition of two whistler mode waves, $\mathbf{B}_\omega^+$ and $\mathbf{B}_\omega^-$, propagating parallel and anti-parallel to the background magnetic field, respectively (for the coordinate system see Fig. 1). The waves $\mathbf{B}_\omega^+$ and $\mathbf{B}_\omega^-$ are written as:

$$\mathbf{B}_\omega^+ = +B_\omega \cos(kx-\omega t)\hat{\mathbf{y}} - B_\omega \sin(kx-\omega t)\hat{\mathbf{z}}, \tag{1}$$

$$\mathbf{B}_\omega^- = +B_\omega \cos(-kx-\omega t+\theta_0)\hat{\mathbf{y}} - B_\omega \sin(-kx-\omega t+\theta_0)\hat{\mathbf{z}}, \tag{2}$$

where B_ω is the whistler wave amplitude, θ_0 is the initial phase difference of the waves and ω and k are the wave frequency and wave number of the whistler waves, related by the electron whistler mode dispersion relation (neglecting ion effects)

$$\frac{k^2c^2}{\omega^2} = 1 - \frac{\omega_{pe}^2}{\omega(\omega-\Omega_e)}, \tag{3}$$

where ω_{pe} is the plasma oscillation frequency and $\Omega_e = eB_0/m$ is the electron gyrofrequency. The corresponding electric field is obtained from Maxwell's relation for plane propagating waves: $k\mathbf{E}_\omega = \omega\hat{\mathbf{k}}\wedge\mathbf{B}_\omega$. Each of the whistler mode waves is in resonance with electrons traveling anti-parallel to its wave number $\mathbf{k}$, with resonance velocity, $\mathbf{v_r}$, given by the resonance condition

$$\omega - \mathbf{k}\cdot\mathbf{v}_r = n\Omega_e/\gamma, \tag{4}$$

where n is an integer and $\gamma = (1-v^2/c^2)^{-1/2}$ is the relativistic factor, which is not constant since electrons can gain or lose energy through the interaction with the whistler waves.

We substitute the fields into the Lorentz Force Law and derive the following normalized equations of motion (for a more detailed derivation see the Appendix):

$$\frac{dv_\parallel}{dt} = +\frac{bv_\perp}{\gamma}\left(1-\frac{v_\parallel}{c^2}\right)\sin\psi + \frac{bv_\perp}{\gamma}\left(1+\frac{v_\parallel}{c^2}\right)\sin(\psi+\Delta\psi), \tag{5}$$

TABLE I. Values of the electron gyrofrequency, Ω_e, wave frequency, ω, plasma frequency, ω_{pe}, magnetic-field strength, B_0, and wave amplitude, B_ω, given for both the Terrestrial (see, for example, Refs. 22–24) and Jovian (Refs. 16 and 17) magnetospheres. The two planetary magnetospheres have quantitatively similar parameters in the normalized system.

Parameter	Earth $L=6.6$	Jupiter $L=6$	Normalized parameter	Earth $L=6.6$	Jupiter $L=6$
Ω_e (kHz)	25.3	334	⋯	1	1
ω (kHz)	0–25.3	0–334	ω/Ω_e	0–1	0–1
ω_{pe} (kHz)	184	2231	ω_{pe}/Ω_e	7.25	7.1
B_0 (nT)	144	1900	⋯	1	1
B_ω (pT)	400	1	B_ω/B_0	10^{-3}–10^{-4}	10^{-6}

$$\frac{dv_\perp}{dt}=-\frac{b}{\gamma}\left[v_\parallel-\left(1+\frac{v_\perp^2}{c^2}\right)\right]\sin\psi - \frac{b}{\gamma}\left[v_\parallel+\left(1+\frac{v_\perp^2}{c^2}\right)\right]\sin(\psi+\Delta\psi), \tag{6}$$

$$\frac{d\psi}{dt}=kv_\parallel-\omega+\frac{1}{\gamma}-\frac{b}{\gamma v_\perp}(v_\parallel-1)\cos\psi - \frac{b}{\gamma v_\perp}(v_\parallel+1)\cos(\psi+\Delta\psi), \tag{7}$$

$$\frac{d\gamma}{dt}=\frac{bv_\perp}{c^2}\sin\psi_1-\frac{bv_\perp}{c^2}\sin(\psi+\Delta\psi), \tag{8}$$

where $b=B_\omega/B_0$ is the normalized wave amplitude, time has been normalized to the electron gyroperiod and $v_\parallel$ and $v_\perp$ are the velocities parallel and perpendicular to the background field, respectively, normalized to the phase velocity of the waves, $v_\phi=\omega/k$. The phase angle, ψ, is the angle between the perpendicular velocity and the waves propagating in the positive $\hat{\mathbf{x}}$ direction, given in the plane perpendicular to the background field and the phase difference, $\Delta\psi=\theta_0-2kx$, is the angle between the two waves. Again, for the geometry, see Fig. 1. For clarity, we refer to Eqs. (5)–(8) as the full equations of motion.

A. Numerical results

The full equations, (5)–(8), are solved numerically using a variable order, variable step size differential equation integrator (see Refs. 11 and 12). We present numerical solutions of the full equations using phase space diagrams. These are composed of a sum of stroboscopic surfaces of section (see Ref. 13) to sample the full electron phase space.

1. Physical parameters used in the numerical solutions

Electron–whistler interactions are considered at $L\simeq 6.6$ in the Terrestrial magnetosphere (geo-synchronous orbit) due to the abundance of experimental data and in the Io torus in the Jovian magnetosphere (at about 6 Jovian radii), a region of increased wave power and electron energy. Physical parameters are shown in Table I. Scaling the physical parameters to intrinsic magnetospheric quantities (see normalization in the Appendix) gives normalized parameters for the Terrestrial and Jovian magnetospheres that are quantitatively similar. We therefore consider a generalized magnetosphere with wave frequencies up to the electron gyrofrequency, wave amplitudes of the order of 2×10^{-6} for quiet times increasing by up to an order of magnitude during intense magnetospheric activity and a plasma frequency in the range 7.1–7.25.

2. Numerical solutions of the full equations

The numerical solutions of the full equations have been presented in detail for the nonrelativistic case in Ref. 7 and for the relativistic case in Ref. 8, therefore, only the important aspects of the solutions are briefly reiterated here.

The initial pitch angle was varied over the range [0°, 180°], so that the initial parallel velocity covers the range $[-v_r,v_r]$, where v_r is the resonance velocity, given by the resonance condition, (4), for $n=1$. As expected from (5) to (8), and as shown in the following analysis, an order parameter is $bv_\perp$, and hence high pitch angles, $v_\perp \gg v_\parallel$, are more likely to exhibit stochasticity at the wave amplitudes seen typically in magnetospheres. Distribution functions with a high perpendicular velocity anisotropy (''pancake'' distributions) are also typically required by gyroresonant diffusion mechanisms and in plasma density models to fit observations.[14] The initial x coordinate (distance along the background field) was chosen so that the initial phase angle $\psi(t=0)$ (angle between the perpendicular velocity and the first whistler wave B_ω^+, see Fig. 1) was either 0 or π.

Figures 2(a) and 2(c) show that the degree of stochasticity increases with the normalized wave amplitude, $b=B_\omega/B_0$ [Figs. 2(b) and 2(d) are explained in Sec. II B]. Initially almost all trajectories are regular [Fig. 2(a), $b=0.001$] and are confined to Kolomogorov–Arnold–Moser (KAM) surfaces (near-integrable trajectories with an approximate constant of the motion, see e.g., Ref. 13). Stochastic trajectories appear as the wave amplitude is increased and the regular orbits between the two resonances are progressively destroyed. The stochastic region grows and further erodes the KAM surfaces close to the resonances [Fig. 2(c), $b=0.005$]. The stochastic region is bounded by the first untrapped (regular) trajectories away from the resonances, thus there is a limit on diffusion in phase space.

In Fig. 3(a) we plot the pitch angle, α in degrees, against phase angle, ψ in radians, with the same parameters as in Fig. 2(c); i.e., $b=0.005$, $\omega=\Omega_e/3$, $E=340$ keV. Phase space is divided into stochastic and regular regions in a similar way. Regular trajectories are confined to close to the resonance pitch angle, $\alpha_r=\arctan(v_{\perp,0}/v_r)$. Stochastic electrons can diffuse throughout the stochastic region and undergo larger changes in pitch angle. In Figs. 3(b)–3(d) the pitch angle is plotted as a function of time for electron trajectories in different regions of phase space. In Fig. 3(b) the electron is on resonance. The trajectory is regular with little change in pitch angle. In Fig. 3(c) the electron trajectory is on a regular trajectory, with regular fluctuations in pitch angle. In Fig. 3(d) the electron trajectory is in the stochastic region of phase space. Large, irregular changes in pitch angle occur as the electron diffuses through the stochastic region of phase space.

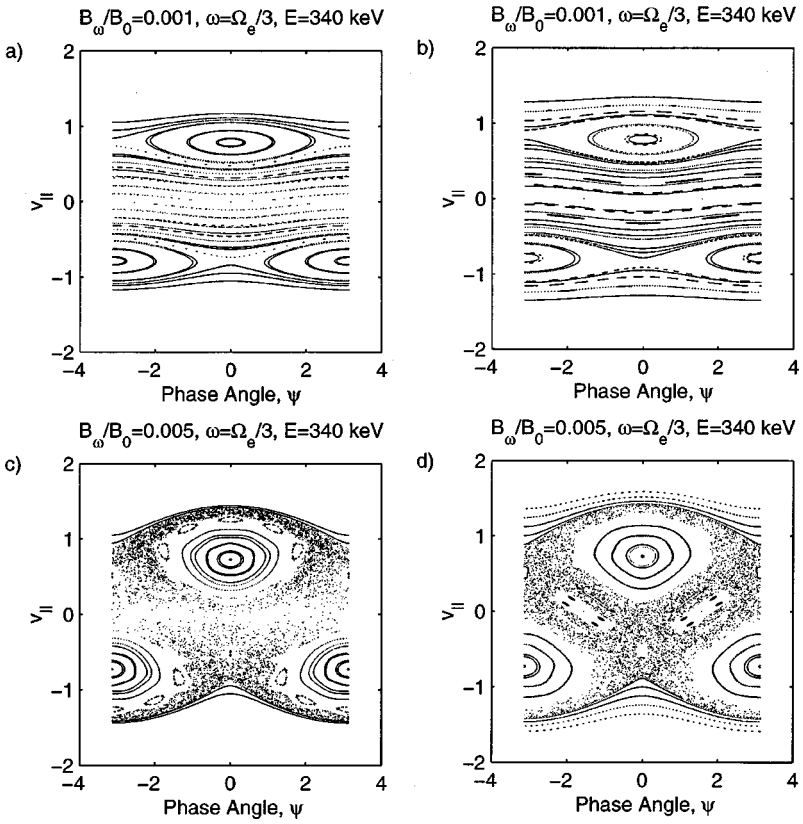

FIG. 2. Stroboscopic surface of section plots for $\omega=\Omega_e/3$, electron energy $E=340$ keV calculated from numerical solutions of the full equations of motion [panels (a) and (c)] and reduced equation [panels (b) and (d)]. For low wave amplitudes [panels (a) and (b), $b=0.001$] all trajectories are regular. At higher wave amplitudes [panels (c) and (d), $b=0.005$] stochastic effects are introduced. Regular trajectories are confined to close to the resonance velocity. The stochastic region is bounded above and below by the first regular, untrapped trajectories away from resonance. Stochastic electrons can diffuse throughout the stochastic region of phase space.

In Figs. 2 and 3, for sufficiently large amplitude whistlers, the region of phase space away from the resonances becomes stochastic. Electrons not in resonance with either of the waves are not restricted to KAM surfaces and can diffuse extensively in the stochastic region of phase space and it is possible to estimate a phase space and thus a pitch angle diffusion coefficient for the diffusion of electrons on a stochastic trajectory. Dynamics in the vicinity of resonance are unchanged.

B. Reduced equations

Since the observed wave amplitude is generally much less than the background magnetic-field strength equations (5)–(8) can be approximated in the limit $b \ll 1$. We assume small perturbations in the velocities of the order of b:

$$v_\parallel = v_{\parallel,0} + b v_{\parallel,1}, \tag{9}$$

$$v_\perp = v_{\perp,0} + b v_{\perp,1}. \tag{10}$$

Then to first order in b we have

$$\frac{dv_{\parallel,0}}{dt} = 0, \tag{11}$$

$$\frac{dv_{\perp,0}}{dt} = 0, \tag{12}$$

thus $v_{\parallel,0}$ and $v_{\perp,0}$ are the constant initial parallel and perpendicular velocities. Taking Eq. (7) to lowest order and integrating once gives

$$\psi = (1/\gamma_0 - \omega)t + kx, \tag{13}$$

$$\psi + \Delta\psi = (1/\gamma_0 - \omega)t - kx + \theta_0. \tag{14}$$

Since $d\gamma/dt \sim b$, the relativistic factor $\gamma_0 = \sqrt{1 - v_{\parallel,0}^2/c^2 - v_{\perp,0}^2/c^2}$ is a constant. To the next order in b:

$$\frac{dv_{\parallel,1}}{dt} = + \frac{v_{\perp,0}}{\gamma}\left(1 - \frac{v_{\parallel,0}}{c^2}\right)\sin\psi + \frac{v_{\perp,0}}{\gamma}\left(1 + \frac{v_{\parallel,0}}{c^2}\right)\sin(\psi + \Delta\psi), \tag{15}$$

which may be written using (13) and (14) in the limit $v_{\parallel,0} \ll c^2$ as

$$\frac{d^2x}{dt^2} = + \frac{b v_{\perp,0}}{\gamma_0}\sin[(1/\gamma_0 - \omega)t + kx] + \frac{b v_{\perp,0}}{\gamma_0}\sin[(1/\gamma_0 - \omega)t - kx + \theta_0], \tag{16}$$

where $v_{\perp,0}$ is the initial perpendicular velocity and $\gamma_0 = 1/\sqrt{(1 - v_{\parallel,0}^2/c^2 - v_{\perp,0}^2/c^2)}$. For clarity we shall refer to Eq. (16) as the reduced equation. The reduced equation has the form of two coupled pendula, with perturbations proportional to $b v_{\perp,0}/\gamma_0$.

1. Numerical solutions of the reduced equation

Numerical solutions of the reduced equation are shown in Figs. 2(b) and 2(d), for the same parameters as Figs. 2(a) and 2(c). These can be seen to yield phase space diagrams that are qualitatively similar to those of the full equations. The reduced equation has the form of two coupled pendula with coordinates $\dot{x}$ and x [these are related to $v_\parallel$ and ψ since

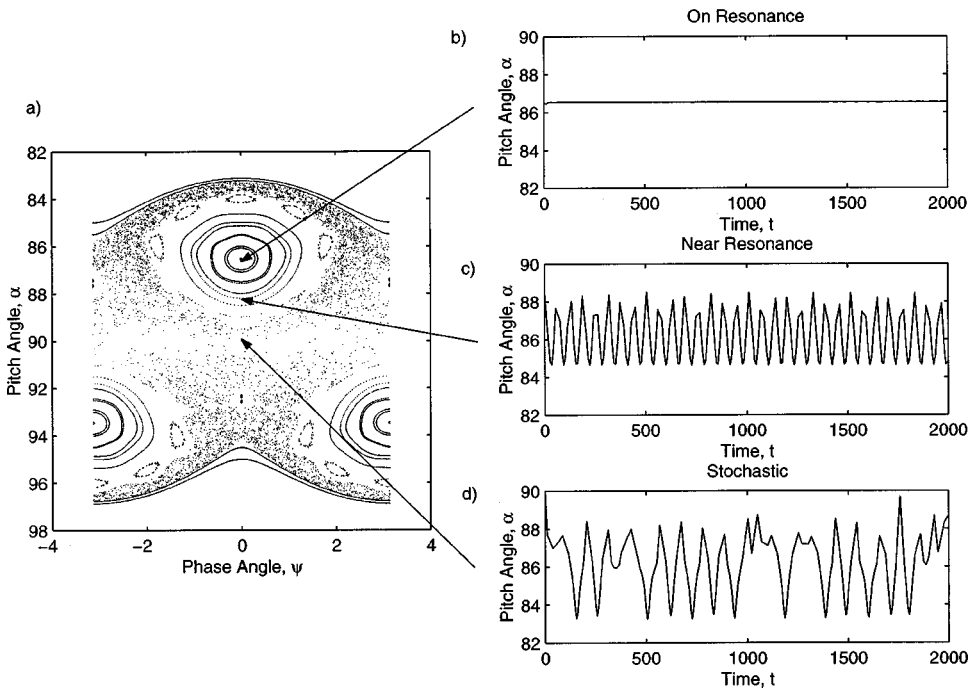

FIG. 3. In panel (a) electron pitch angle in degrees in plotted against phase angle. Parameters are as in Fig. 2(c), i.e., $\omega=\Omega_e/3$, $b=0.005$ and $E=340$ keV. The phase plots are qualitatively similar and share many of the same features. In panels (b)–(d) the pitch angle is plotted as a function of time. In panel (b) the electron is on resonance with little change in pitch angle. In panel (c) the electron is on a regular trajectory, with the pitch angle changing regularly with time. In panel (d) the electron trajectory is stochastic with larger, irregular changes in pitch angle.

$v_\parallel=\dot{x}$ and $\psi=kx+(1/\gamma_0-\omega)t)]$. The amplitude of oscillation is proportional to $bv_{\perp,0}/\gamma_0$. There is a transition to stochasticity as the amplitude of oscillation increases. This is demonstrated in Fig. 2, where the system becomes stochastic as b is increased, from $b=0.001$ [Fig. 2(b)] to $b=0.005$ [Fig. 2(d)].

The reduced equation (16), therefore, preserves the underlying dynamics of the full system of equations [Eq. (5)–(8)] but allows us to consider a simpler system which is readily extended to a more realistic case, i.e., wave packets, which we present in the next section.

III. BROAD BAND WHISTLERS

A. Single wave packet

Using the framework established in Sec. II we can extend the reduced equation (16) to consider broad band whistler wave packets. We express the wave number in terms of the wave frequency, using the derivatives of the linearized dispersion relation (3), evaluated at the central wave frequency, ω_0, and wave number, k_0, of the wave packet

$$k(\omega)=k_0+\left.\frac{dk}{d\omega}\right|_{\omega_0,k_0}(\omega-\omega_0)+\left.\frac{d^2k}{d\omega^2}\right|_{\omega_0,k_0}(\omega-\omega_0)^2+\cdots. \tag{17}$$

Assuming the first derivative is approximately constant over the width of the wave packet we can write $k=k_0+(\omega-\omega_0)/v_g$, where $v_g=d\omega/dk$ is the group velocity of the wave, evaluated at $\omega=\omega_0$ and $k=k_0$. We parameterize the wave frequency, wave number, and wave amplitude in terms of an integer, n, and a finite bandwidth, $\Delta\omega$, i.e., $\omega_n=\omega_0+n\Delta\omega$, $k_n=k_0+n\Delta k=\omega_0+n\Delta\omega/v_g$ and $b_n=b$. The reduced equation for a single wave becomes

$$\frac{d^2x}{dt^2}=+\frac{v_{\perp,0}}{\gamma_0}\sin[(1/\gamma_0-\omega)t+kx]f_n(r), \tag{18}$$

where

$$f_n(r)=b_ne^{-i(\omega_n-\omega_0)r}, \tag{19}$$

and we have written $r=t-x/v_g$. We now consider the interaction with an infinite series of monochromatic waves each centered at wave frequency, ω_n, with amplitude, b_n, where $n\in[-\infty,\infty]$. Equation (18) becomes

$$\frac{d^2x}{dt^2}=+\frac{v_{\perp,0}}{\gamma_0}\sin[(1/\gamma_0-\omega_0)t+k_0x]f(r), \tag{20}$$

where

$$f(r)=\sum_{n=-\infty}^{\infty}b_ne^{-i(\omega_n-\omega_0)r}. \tag{21}$$

Equation (20) is expressed as a Fourier series with coefficients b_n. From the definition of Fourier transforms (given in Ref. 15) we obtain

$$f(r)=\int_{-\infty}^{\infty}A(\omega)e^{-i(\omega-\omega_0)r}d\omega, \tag{22}$$

$$A(\omega)=\frac{1}{2\pi}\int_{-\infty}^{\infty}f(r)e^{i(\omega-\omega_0)r}dr. \tag{23}$$

Equations (22) and (23) are now a Fourier transform pair. The function $A(\omega)$ represents the wave amplitude per unit

wave frequency bandwidth. Depending on the form of $A(\omega)$ we can solve Eq. (22) and determine the approximate equation of motion for a single wave packet.

1. Delta function

For monochromatic waves we can write $A(\omega)$ in terms of a δ-function centered at frequency ω_0

$$A(\omega)=b_0\delta(\omega-\omega_0). \tag{24}$$

Equation (22) is readily integrated to give $f(r)=b_0$ and Eq. (20) becomes

$$\frac{d^2x}{dt^2}=+\frac{b_0 v_{\perp,0}}{\gamma_0}\sin[(1/\gamma_0-\omega_0)t+k_0x], \tag{25}$$

which is the reduced equation for a single monochromatic whistler.

B. Scattering due to a single wave packet

We can write the function, $A(\omega)$, as a top hat distribution, i.e. the wave amplitude is constant over a finite frequency range and zero everywhere else:

$$A(\omega)=\begin{cases} 0 & : \quad \omega<\omega-\Delta\omega/2 \\ A_0 & : \quad \omega-\Delta\omega/2<\omega<\omega+\Delta\omega/2 \\ 0 & : \quad \omega>\omega+\Delta\omega/2 \end{cases}. \tag{26}$$

Solving for $f(r)$ in Eq. (22) and substituting into Eq. (20) gives the following equation of motion:

$$\frac{d^2x}{dt^2}=\frac{v_{\perp,0}}{\gamma_0}A(x,t)\Delta\omega\sin[(1/\gamma_0-\omega_0)t+k_0x], \tag{27}$$

where $A(x,t)$ is given by

$$A(x,t)=A_0\frac{\sin[(x-v_g t)(\Delta\omega/2v_g)]}{(x-v_g t)(\Delta\omega/2v_g)}. \tag{28}$$

If the extrema of the packet wave frequencies and wave numbers are given by $\omega^{\pm}=\omega_0\pm\Delta\omega/2$ and $k^{\pm}=k_0\pm\Delta k/2$ then Eq. (27) can be written as:

$$\frac{d^2x}{dt^2}=+\frac{A_0}{(t-x/v_g)}\frac{v_{\perp,0}}{\gamma_0}\cos[(1/\gamma_0-\omega^+)t+k^+x] + \frac{A_0}{(t-x/v_g)}\frac{v_{\perp,0}}{\gamma_0}\cos[(1/\gamma_0-\omega^-)t+k^-x+\pi], \tag{29}$$

which we compare with the reduced equation for two waves with frequencies ω^+ and ω^- [obtained by defining $A(\omega)=b_0\delta(\omega-\omega^+)+b_0\delta(\omega-\omega^-)$ in Eq. (22)]:

$$\frac{d^2x}{dt^2}=+\frac{b_0 v_{\perp,0}}{\gamma_0}\sin[(1/\gamma_0-\omega^+)t+k^+x] + \frac{b_0 v_{\perp,0}}{\gamma_0}\sin[(1/\gamma_0-\omega^-)t+k^-x]. \tag{30}$$

The two equations are qualitatively similar, differing only in the phase difference in the sine and cosine terms (but see Ref. 7) and the wave amplitudes. Therefore, we conclude that a single wave packet scatters electrons in phase space as if it were composed of a pair of monochromatic whistlers with an enhanced wave amplitude given by $A_0/(t-x/v_g)$. We expect that a single broad band wave packet will result in the diffusion of stochastic electrons in a similar way to two oppositely directed monochromatic whistlers.

1. Gaussian wave amplitude distribution

Instead of a top hat distribution, the function, $A(\omega)$, can be written as a Gaussian distribution of width $\Delta\omega$, with magnitude, A_0, and central wave frequency, ω_0

$$A(\omega)=A_0 e^{-(\omega-\omega_0)^2/\Delta\omega^2}. \tag{31}$$

Substituting $A(\omega)$ into Eq. (22) and integrating over all wave frequencies gives $f(r)$, which is then substituted into Eq. (20) to give the equation of motion for the interaction with a single wave with a Gaussian wave amplitude distribution

$$\frac{d^2x}{dt^2}=\frac{v_{\perp,0}}{\gamma_0}A(x,t)\Delta\omega\sin[(1/\gamma_0-\omega_0)t+k_0x], \tag{32}$$

where $A(x,t)$ is given by

$$A(x,t)=A_0 e^{-(x-v_g t)^2(\Delta\omega/2v_g)^2}. \tag{33}$$

We define the wave density, A_0, as the wave amplitude per unit wave frequency bandwidth, with units of Teslas per Hertz. In the limit where the width of the wave packet tends to zero, the Gaussian wave packet becomes a δ-function. Hence (32) yields the reduced equation (16) in the limit where $\Delta\omega\to 0$ provided A_0 satisfies

$$\lim_{\Delta\omega\to 0}\frac{A_0}{\Delta\omega}=b_0. \tag{34}$$

C. Oppositely directed wave packets

We have shown that the scattering due to a single wave packet can be described as effectively that due to the interaction of two monochromatic whistlers with enhanced wave amplitudes [see Eq. (29)]. In order to find the maximal degree of stochasticity in the system two oppositely directed wave packets are considered. The equation of motion for two wave packets, with Gaussian wave amplitude distribution, is derived in a similar way to Eq. (32)

$$\frac{d^2x}{dt^2}=+\frac{v_{\perp,0}}{\gamma_0}A^+(x,t)\Delta\omega\sin[(1/\gamma_0-\omega_0)t+k_0x] + \frac{v_{\perp,0}}{\gamma_0}A^-(x,t)\Delta\omega\sin[(1/\gamma_0-\omega_0)t-k_0x], \tag{35}$$

where $A^+(x,t)$ and $A^-(x,t)$ are given by

$$A^+(x,t)=A_0 e^{-(x-v_g t)^2(\Delta\omega/2v_g)^2}, \tag{36}$$

$$A^-(x,t)=A_0 e^{-(x+v_g t)^2(\Delta\omega/2v_g)^2}. \tag{37}$$

Equation (35) is referred to as the wave packet equation.

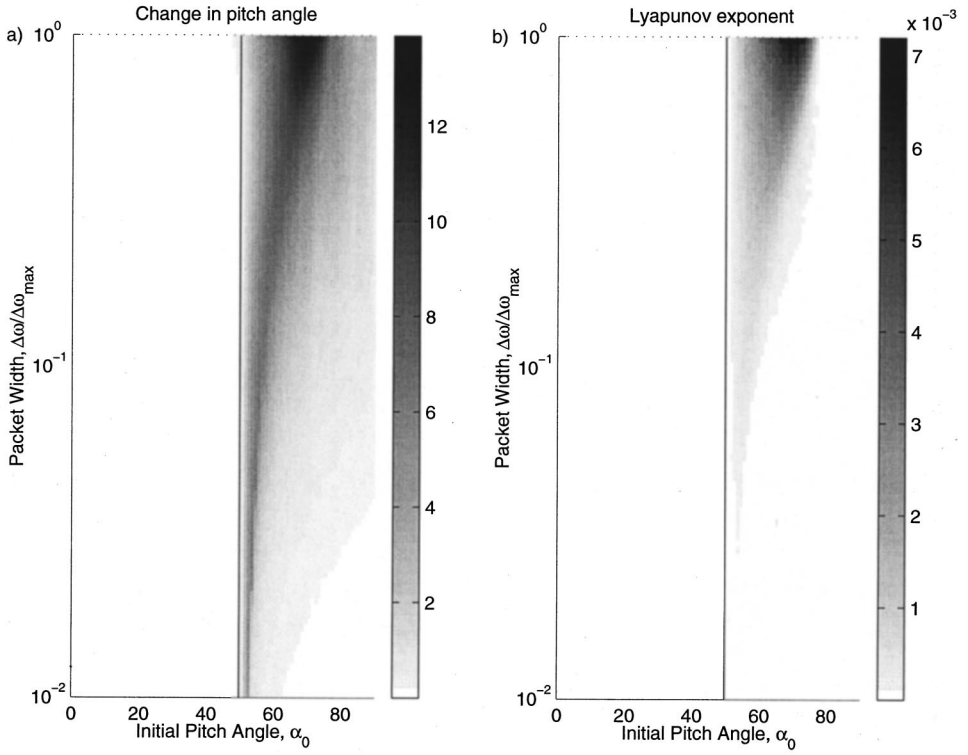

FIG. 4. In panel (a) the change in pitch angle in degrees is calculated for electrons interacting with a range of wave packet widths ($E=80$ keV, $\omega=\Omega_e/10$). For narrow wave packets the change in pitch angle is maximum for regular trajectories [zero Lyapunov exponent in panel (b)] close to resonance (indicated by the vertical black line). For wide wave packets the maximum change in pitch angle occurs for electrons in the stochastic region of phase space [positive Lyapunov exponent in panel (b)] away from resonance.

D. Numerical solutions of wave packet equation

The wave density, A_0, is estimated from the analysis of Voyager 1 data (see Refs. 16–18) for the Jovian magnetosphere

$$A_0=\frac{b_0}{\Delta\omega_i}=\sqrt{\frac{B'}{\Delta\omega_i}}, \tag{38}$$

where B' is the magnetic-field spectral density (in units of T^2/Hz^{-1}) and $\Delta\omega_i$ is the instrument bandwidth at a given frequency. For all frequencies up to the gyrofrequency $A_0 \approx 2\times10^{-3}$. For the generalized magnetosphere we assume $A_0\approx2\times10^{-3}$ is a good estimate for undisturbed times and additionally consider enhancements of up to an order of magnitude for intense magnetospheric events such as substorms.

E. Lyapunov exponent

We quantify the degree of stochasticity in the system by considering Lyapunov exponents of numerical solutions of the wave packet equation (35), for a given set of parameters (wave density, wave frequency, and electron energy). The Lyapunov exponents are estimated using the method described in Refs. 19 and 20. The Lyapunov exponents are estimated over all phase space and evolved to their asymptotic limit. The only significant Lyapunov exponent corresponds to spatial perturbations along the background field direction. A positive Lyapunov exponent corresponds to a stochastic trajectory while a zero Lyapunov exponent indicates the trajectory is regular. For a thorough description of Lyapunov exponents see Ref. 21.

F. Pitch angle diffusion

It is not possible to produce phase space diagrams for the wave packet equations due to their implicit time dependence. Instead other methods are used to analyze them. In Fig. 4 we consider the interaction between 80 keV electrons with initial pitch angles in the range [0°, 90°] and two oppositely directed whistler wave packets with wave frequency, $\omega=\Omega_e/10$ and wave packet widths up to the maximum for a given frequency, $\Delta\omega_{\max}$. The maximum packet width $\Delta\omega_{\max}$ is chosen to be as large as possible, providing that the extrema of the wavepacket frequencies given by $\omega^{\pm}=\omega_0\pm\Delta\omega/2$ does not exceed the limits of either zero or the electron gyrofrequency. Finally, we consider an enhanced wave density, $A=10A_0$, to represent intense magnetospheric activity.

In Fig. 4(a) we consider the change in pitch angle in degrees for increasing wave packet widths. In Fig. 4(b) we plot the dimensionless (i.e., normalized) Lyapunov exponent $\lambda^*=\lambda\Omega_e^{-1}$. For narrow bandwidths, $\Delta\omega/\Delta\omega_{\max}=10^{-2}$, the wave packet equation yields the reduced equation with low wave amplitudes. The maximum change in pitch angle occurs for regular electron trajectories [indicated by zero Lyapunov exponent in Fig. 4(b)] close to resonance (indicated by the vertical black line at $\alpha_0=50°$). As the wave packet width increases stochastic effects (in the dynamical sense) are introduced, as indicated by positive Lyapunov exponent in Fig. 4(b). Significant change in pitch angle occurs, due to stochastic interactions, for electrons away from resonance. As the wave packet width approaches $\Delta\omega_{\max}$, diffusion is maximum in the stochastic regions of phase space.

In Fig. 5 we show the regions of phase space where the diffusion of stochastic electrons occurs, as a function of both

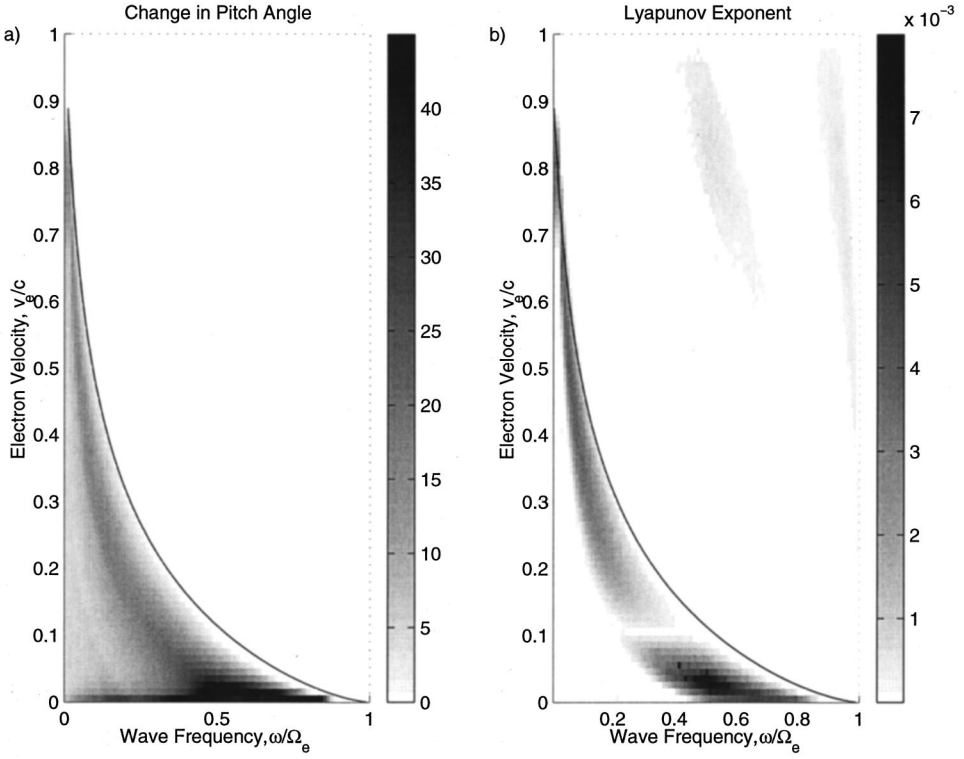

FIG. 5. In panel (a) we show the electron velocities and wave frequencies for which a significant change in pitch angle (in degrees) occurs. Pitch angle diffusion is maximum for stochastic electrons [indicated by positive Lyapunov exponent in panel (b)]. The stochastic region of phase space occurs away from resonance (indicated by the black line in both panels).

electron energy and wave frequency. Maximum change in pitch angle (in degrees) occurs away from resonance (indicated by the black lines in both panels) due to stochastic interactions [positive Lyapunov exponent in Fig. 5(b)].

IV. DIFFUSION COEFFICIENT

In this section we estimate the pitch angle diffusion coefficient for the scattering of electrons at resonance in a random background of wave fluctuations (see Ref. 1), D_{KP}, compared with the diffusion coefficient for stochastic (in the dynamical sense) electrons, D_L, estimated from the solutions of the wave packet equation. The diffusion coefficient for the gyroresonant interaction with a single whistler is given in Ref. 1 (page 13 onwards)

$$D_{KP} \approx \frac{(\Delta\alpha)^2}{2\Delta t} \approx \left(\frac{B_\omega}{B_0}\right)^2 \frac{\Omega_e^2 \Delta t}{2}, \tag{39}$$

where $\Delta t \approx 2/\Delta k v_\parallel$ is the time a particle is in resonance with the wave.

For two oppositely directed broad band whistlers, the Lyapunov exponent estimated here can be used to estimate a diffusion coefficient. The separation of two electrons with Lyapunov exponent, λ, in phase space, scales approximately as $\sim \exp \lambda t$, thus an order of magnitude estimate shows that changes in pitch angle scale approximately as $\sim \exp \lambda t$, giving a characteristic time constant, τ, for changes in pitch angle of by a factor of e^1, of approximately $\tau \sim 1/\lambda$ gyroperiods. In Figs. 4 and 5 the maximum Lyapunov exponent is of the order of 10^{-2}–10^{-3}. This implies that the changes in pitch angle occur on time scales of the order of 10^2–10^3 electron gyroperiods. This indicates very short interaction times (less than one second) and hence confirms the validity of the approximation of constant background magnetic field.

Since changes in pitch angle of the order of $\Delta\alpha = e^1$ occur on time scales of the order of $\Delta t = 1/\lambda$ (where we obtain the un-normalized Lyapunov exponent from $\lambda = \lambda^* \Omega_e$), the normalized diffusion coefficient can be estimated as

$$D_L \approx \frac{(\Delta\alpha)^2}{2\Delta t} \approx \frac{1}{2} e^2 \lambda^* \Omega_e . \tag{40}$$

Thus the diffusion coefficient scales with the electron gyrofrequency and has units of radians^2 s^{-1}. We estimate the diffusion coefficients for resonant diffusion and stochastic diffusion in both magnetospheres in Tables II and III, for broadband ($\Delta\omega \approx \omega$) low-frequency ($\omega = \Omega_e/10$) waves interacting with 80 keV electrons. Note that the same wave density corresponds to different wave amplitudes in the different magnetospheres.

In the Terrestrial magnetosphere (Table II) at low wave densities ($A_0 = 10^{-4}$) the stochastic diffusion mechanism is not ''switched on,'' resulting in zero diffusion coefficient and infinite diffusion time scales. The dominant diffusion

TABLE II. Estimated diffusion coefficients, diffusion time scales (for resonant and stochastic diffusion) and bounce time scales for the Terrestrial magnetosphere, for increasing wave density and wave amplitude.

A_0	B_ω/B_0	D_{KP}	τ_{KP}	D_L	τ_L	τ_b
10^{-4}	2×10^{-6}	2×10^{-6}	5×10^{5}	0	∞	1
10^{-3}	2×10^{-5}	2×10^{-4}	5×10^{3}	10^{-1}	10	1
10^{-2}	2×10^{-4}	2×10^{-2}	50	1	1	1
10^{-1}	2×10^{-3}	2	0.5	10	10^{-1}	1

TABLE III. Estimated diffusion coefficients, diffusion time scales (for resonant and stochastic diffusion) and bounce time scales for the Jovian magnetosphere, for increasing wave density and wave amplitude.

A_0	B_ω/B_0	D_{KP}	τ_{KP}	D_L	τ_L	τ_b
10^{-4}	10^{-7}	10^{-8}	10^{8}	0	∞	10
10^{-3}	10^{-6}	10^{-6}	10^{6}	1	1	10
10^{-2}	10^{-5}	10^{-4}	10^{4}	10	10^{-1}	10
10^{-1}	10^{-4}	10^{-2}	10^{2}	100	10^{-2}	10

mechanism is resonant diffusion albeit with diffusion time scales of the order of several days ($\tau_{KP} \ll \tau_b$). For larger wave densities the stochastic diffusion mechanism is switched on resulting in diffusion coefficients initially an order of magnitude greater than for resonant diffusion. Comparing the time scale for diffusion by one radian with the bounce time scale we find that stochastic diffusion is significant for wave densities greater than the quiet time wave density ($A \geqslant A_0 = 10^{-3}$). A similar result is obtained for the Jovian magnetosphere (Table III) except that the diffusion coefficients for resonant diffusion are generally an order of magnitude higher.

V. DISCUSSION

The interaction between relativistic electrons and two oppositely directed monochromatic whistler waves is stochastic (in the dynamical sense) for sufficiently large wave amplitudes. Stochastic electrons can diffuse throughout the stochastic region resulting in electron diffusion in phase space. Regular orbits still exist close to resonance, hence their dynamics is unchanged from that found for a single monochromatic wave.

An analytical description of wave packets was derived to consider broadband whistler waves. Stochastic trajectories were shown to exist and it was found that a single broad band whistler wave packet scatters electrons as if it were effectively composed of two oppositely directed monochromatic whistlers with enhanced wave amplitude. Diffusion of stochastic electrons occurred for low wave amplitudes consistent with the Terrestrial and Jovian magnetospheres.

The degree of stochasticity in the system was quantified by considering the Lyapunov exponent of solutions of the wave packet equation. Significant pitch angle diffusion occurs for stochastic electrons, whose trajectories have positive Lyapunov exponent. Given the Lyapunov exponent one can obtain an estimate for the pitch angle diffusion coefficient; this is found to be significant during conditions of enhanced magnetospheric activity.

ACKNOWLEDGMENTS

W.J.W. was funded by a PPARC studentship and S.C.C. by a PPARC fellowship.

APPENDIX: DERIVATION OF THE FULL EQUATION OF MOTION

The wave field is described by a vector potential

$$\mathbf{A}_\omega = + \frac{B_\omega}{k}(\cos(kx-\omega t) - \cos(-kx-\omega t+\theta_0))\hat{\mathbf{y}} - \frac{B_\omega}{k}(\sin(kx-\omega t) - \sin(-kx-\omega t+\theta_0))\hat{\mathbf{z}}, \quad \text{(A1)}$$

giving magnetic ($\mathbf{B}_\omega = \nabla \times A_\omega$) and electric ($\mathbf{E}_\omega = -dA_\omega/dt$) wave fields of the form

$$\mathbf{B}_\omega^+ = + B_\omega \cos(kx-\omega t)\hat{\mathbf{y}} - B_\omega \sin(kx-\omega t)\hat{\mathbf{z}}, \quad \text{(A2)}$$

$$\mathbf{B}_\omega^- = + B_\omega \cos(-kx-\omega t+\theta_0)\hat{\mathbf{y}} - B_\omega \sin(-kx-\omega t+\theta_0)\hat{\mathbf{z}}, \quad \text{(A3)}$$

$$\mathbf{E}_\omega^+ = - B_\omega \frac{\omega}{k}\sin(kx-\omega t)\hat{\mathbf{y}} + B_\omega \frac{\omega}{k}\cos(kx-\omega t)\hat{\mathbf{z}}, \quad \text{(A4)}$$

$$\mathbf{E}_\omega^- = + B_\omega \frac{\omega}{k}\sin(-kx-\omega t+\theta_0)\hat{\mathbf{y}} + B_\omega \frac{\omega}{k}\cos(-kx-\omega t+\theta_0)\hat{\mathbf{z}}. \quad \text{(A5)}$$

The velocity is written in terms of its components parallel and perpendicular to the background magnetic field; $\mathbf{v} = v_\parallel \hat{\mathbf{x}} + v_\perp \cos\phi \hat{\mathbf{y}} + v_\perp \sin\phi \hat{\mathbf{z}}$, where $\phi = \phi(t)$ is the phase of the perpendicular velocity with respect to the $\hat{\mathbf{y}}$ axis. The phase angle $\psi = kx - \omega t + \phi$ is defined as the angle between the perpendicular velocity and $\mathbf{B}_\omega^+$ and the phase difference $\Delta\psi = \theta_0 - 2kx$ as the angle between the two waves.

Substituting into the relativistic Lorentz Force Law gives the following equations of motion (in the frame in which the waves have phase speeds, $v_\phi^\pm = \pm\omega/k$):

$$\frac{dv_\parallel}{dt} = + \frac{eB_\omega v_\perp}{\gamma m}\left(1 - \frac{\omega v_\parallel}{kc^2}\right)\sin\psi + \frac{eB_\omega v_\perp}{\gamma m}\left(1 + \frac{\omega v_\parallel}{kc^2}\right)\sin(\psi+\Delta\psi), \quad \text{(A6)}$$

$$\frac{dv_\perp}{dt} = - \frac{eB_\omega}{\gamma m}\left[v_\parallel - \frac{\omega}{k}\left(1 + \frac{v_\perp^2}{c^2}\right)\right]\sin\psi - \frac{eB_\omega}{\gamma m}\left[v_\parallel + \frac{\omega}{k}\left(1 + \frac{v_\perp^2}{c^2}\right)\right]\sin(\psi+\Delta\psi), \quad \text{(A7)}$$

$$\frac{d\psi}{dt} = kv_\parallel - \omega + \frac{\omega_e}{\gamma} - \frac{eB_\omega}{\gamma m v_\perp}\left(v_\parallel - \frac{\omega}{k}\right)\cos\psi - \frac{eB_\omega}{\gamma m v_\perp}\left(v_\parallel + \frac{\omega}{k}\right)\cos(\psi+\Delta\psi), \quad \text{(A8)}$$

$$\frac{d\gamma}{dt} = \frac{eB_\omega \omega v_\perp}{kmc^2}\sin\psi - \frac{eB_\omega \omega v_\perp}{kmc^2}\sin(\psi+\Delta\psi). \quad \text{(A9)}$$

The model is simplified by making the following normalizations: $b^* = B_\omega/B_0$, $t^* = t\Omega_e$, $x^* = x\Omega_e/v_\phi$, $v^* = v/v_\phi$, $c^* = c/v_\phi$, $\gamma^* = (1 - v^{*2}/c^{*2})^{-1/2}$, $\omega^* = \omega/\Omega_e$, and $k^* = kv_\phi/\Omega_e$ where $v_\phi = \omega/k$ is the phase velocity, which in

the normalized system gives $v_\phi^* = \omega^*/k^* = 1$. Substituting into the above equations and dropping the superscripts gives the normalized equations

$$\frac{dv_\parallel}{dt} = +\frac{bv_\perp}{\gamma}\left(1-\frac{v_\parallel}{c^2}\right)\sin\psi + \frac{bv_\perp}{\gamma}\left(1+\frac{v_\parallel}{c^2}\right)\sin(\psi+\Delta\psi), \tag{A10}$$

$$\frac{dv_\perp}{dt} = -\frac{b}{\gamma}\left[v_\parallel-\left(1+\frac{v_\perp^2}{c^2}\right)\right]\sin\psi - \frac{b}{\gamma}\left[v_\parallel+\left(1+\frac{v_\perp^2}{c^2}\right)\right]\sin(\psi+\Delta\psi), \tag{A11}$$

$$\frac{d\psi}{dt} = kv_\parallel-\omega+\frac{1}{\gamma}-\frac{b}{\gamma v_\perp}(v_\parallel-1)\cos\psi - \frac{b}{\gamma v_\perp}(v_\parallel+1)\cos(\psi+\Delta\psi), \tag{A12}$$

$$\frac{d\gamma}{dt} = \frac{bv_\perp}{c^2}\sin\psi-\frac{bv_\perp}{c^2}\sin(\psi+\Delta\psi). \tag{A13}$$

[1] C. F. Kennel and H. E. Petschek, J. Geophys. Res. **71**, 1 (1966).
[2] L. R. Lyons, R. M. Thorne, and C. F. Kennel, J. Plasma Phys. **77**, 3455 (1972).
[3] R. Gendrin, Rev. Geophys. **19**, 171 (1981).
[4] J. Faith, S. Kuo, and J. Huang, J. Geophys. Res. **102**, 2233 (1997).
[5] U. S. Inan, T. F. Bell, and R. A. Helliwell, J. Geophys. Res., [Space Phys.] **83**, 3235 (1978).
[6] R. A. Helliwell and J. P. Katsufrakis, J. Geophys. Res. **79**, 2571 (1974).
[7] K. S. Matsoukis, S. C. Chapman, and G. Rowlands, Geophys. Res. Lett. **25**, 265 (1998).
[8] W. J. Wykes, S. C. Chapman, and G. Rowlands, Planet. Space Sci. **49**, 395 (2001).
[9] P. E. Devine and S. C. Chapman, Physica D **95**, 35 (1996).
[10] L. R. Lyons and R. M. Thorne, Planet. Space Sci. **18**, 1753 (1970).
[11] L. F. Shampine and M. K. Gordon, *Computer Solution of Ordinary Differential Equations: The Initial Value Problem* (Freeman, New York, 1975).
[12] S. C. Chapman and N. W. Watkins, J. Geophys. Res. **98**, 165 (1993).
[13] M. Tabor, *Chaos and Integrability in Nonlinear Dynamics—An Introduction* (Wiley, Chichester, 1989).
[14] F. J. Crary, F. Bagenal, J. A. Ansher, D. A. Gurnett, and W. S. Kurth, J. Geophys. Res. **101**, 2699 (1996).
[15] T. L. Chow, *Mathematics Methods for Physicists: A Concise Introduction* (Cambridge University Press, Cambridge, 2000).
[16] F. L. Scarf, F. V. Coroniti, D. A. Gurnett, and W. S. Kurth, Geophys. Res. Lett. **6**, 653 (1979).
[17] W. S. Kurth, B. D. Strayer, D. A. Gurnett, and F. L. Scarf, Icarus **61**, 497 (1985).
[18] Y. Hobara, S. Kanemaru, and M. Hayakawa, J. Geophys. Res. **102**, 7115 (1997).
[19] G. Benettin, L. Galgani, and J. M. Strelcyn, Physica A **14**, 2338 (1976).
[20] T. S. Parker and L. O. Chua, *Practical Numerical Algorithms for Chaotic Systems* (Springer-Verlag, New York, 1989).
[21] R. C. Hilborn, *Chaos and Nonlinear Dynamics* (Oxford University Press, Oxford, 1994).
[22] D. Summers and C. Ma, J. Geophys. Res. **105**, 2625 (2000).
[23] M. Parrot and C. A. Gaye, Geophys. Res. Lett. **21**, 2463 (1994).
[24] I. Nagano, S. Yagitani, H. Kojima, and H. Matsumoto, J. Geomagn. Geoelectr. **48**, 299 (1996).